Estuarine, Coastal and Shelf Science 167 (2015) 228–239

Contents lists available at ScienceDirect

Estuarine, Coastal and Shelf Science

journal homepage: www.elsevier.com/locate/ecss

Biochemical and photochemical feedbacks of acute Cd toxicity in *Juncus acutus* seedlings: The role of non-functional Cd-chlorophylls

D. Santos, B. Duarte*, I. Caçador

MARE, Marine and Environmental Sciences Centre, Faculty of Sciences of The University of Lisbon, Campo Grande, 1749-016 Lisbon, Portugal

ARTICLE INFO

Article history:
Received 26 September 2014
Received in revised form
29 September 2015
Accepted 10 October 2015
Available online 22 October 2015

Keywords:
Ecotoxicology
Chlorophyll fluorescence
Heavy metal stress
Halophyte

ABSTRACT

The increasing metal pollution in salt marshes and its influence on the plants that inhabit these ecosystems, has become a major concern with serious implications on the species establishment. *Juncus acutus* is a highly common halophyte specie in Portuguese marshes. Seeds from his specie were exposed to a range of different Cd concentrations (0.05, 0.1, 0.5 and 1 μM) in order to evaluate the effects of acute Cd stress on seed germination and growth as well as on seedling pigment composition, photosynthetic apparatus and oxidative stress biomarkers. Seedling length was higher than in control in every Cd treatment, however biomass showed a decrease. It was also observed that increasing Cd treatments, lead to a proportional increase in the Cd tissue concentration. Also the Cd-substituted chlorophylls showed an increase with increasing Cd doses that were applied. This substitution results in a non-functional chlorophyll molecule, highly unstable under moderate light intensities which inevitably reduces the efficiency of the LHC II. As consequence, there was a decrease in the use-efficiency of the harvested energy, leading to a decay in the photosynthetic capacity and energy accumulation, which was dissipated as heat. As for the antioxidant enzymes, SOD and APX presented higher activity, responding to increasing cadmium concentrations. Thus, becomes evident that Cd affects negatively, both biochemically and photochemically, the establishment by seed process of *J. acutus* highlighting the potential of the use of this specie seed as potential sentinel and ecotoxicity test in extreme conditions.

1. Introduction

Salt marsh ecosystems, as one of the types of wetlands, are of great ecological importance. *Sarcocornia perennis, Sacocornia fruticosa*, *Spartina maritima*, *Halimione portulacoides* (Caçador et al., 1996) and *Juncus acutus* (Martínez-Sánchez et al., 2006; Caçador et al., 2013) are some of the halophyte species which commonly inhabit this environment. Since these ecosystems are located largely near or alongside estuaries, are often exposed and considered as natural sink of heavy metals from industrial and urban sewage (Otte et al., 1991; Caçador et al. 1996). Despite the fact that some species from salt marshes can withstand with some degree of contamination, excessive concentration of metals in the soil can not only cause damages in the plants, but also be potentially harmful to human health, through food chain.

Metals like zinc (Zn), iron (Fe) and nickel (Ni) are essential to plants at lower concentrations with some role in plant physiology, however in excess can cause some disorders. Cadmium (Cd), as other non-essential metals like lead (Pb), is toxic to plants even at low concentrations (Marschner, 1995). Cadmium reaching the estuaries can have several origins. Phosphate fertilizers can present high amounts of cadmium in their composition (Monbet, 2004). Cadmium stored in agricultural soils can be leached during rain events and enter the riverine system. Also, cadmium is very mobile (Duarte et al., 2008), especially in acidic conditions, as the ones promoted by corrective fertilizers. In these conditions leaching is enhanced (Monbet, 2004). On the other hand, industrial activities can also contribute to cadmium introduction to the estuarine ecosystem. This element is widely used in electroplating and galvanizing, as a color pigment in paints and in batteries. It can also be originated as a by-product of zinc and lead mining and smelting (Sandrini et al., 2006). As well as in other estuarine systems, in Tagus estuary Cd presents relatively high concentrations in the sediments (Duarte et al., 2010) and waters (Duarte and Caçador, 2012), being present in highly mobile fraction (Duarte et al., 2008) easily transferred to the food chain (Duarte et al., 2010; Caçador et al., 2012).

* Corresponding author.
E-mail address: baduarte@fc.ul.pt (B. Duarte).

http://dx.doi.org/10.1016/j.ecss.2015.10.005
0272-7714/

Cadmium is an element extremely toxic to organisms, since its solubility in water is very high and has neurotoxic, mutagenic and carcinogenic nature. Its accumulation in plants can be high, due to its great mobility between soil and roots. This non-essential metal leads to photosynthesis inhibition and hinder water and nutrient uptake in the plants causing therefore chlorosis, growth inhibition, ultra-structural damage and ultimately the plant death (Marschner, 1995). High concentration of cadmium in plants can also cause imbalances between production and scavenging of reactive oxygen species, inducing oxidative stress conditions. To counteract the effect of the free radicals, plants had developed a battery of defenses that includes some antioxidant enzymes like superoxide dismutase (SOD), catalase (CAT), guaiacol peroxidase (GPx) and ascorbate peroxidase (APx). These enzymes play an important role in the production of O_2 and H_2O_2, which are less harmful to the organism, from the dismutation of O^{2-} and preventing this way serious cellular damage. In plants cadmium can also substitute the Mg atom at the chlorophyll reaction centre (Küpper et al., 1996). Hence, the formation of minor proportions of [Cd]-Chl relative to the total Chl may already inhibit photosynthesis completely (Küpper et al., 1996).

J. acutus Lam. is a highly common halophyte specie in Portuguese marshes, found in several kinds of sediments from sandy to muddy, gathering this way an increased colonization potential in all sorts of salt marshes (Caçador et al., 2013). Therefore, its widespread presence and wide range of habitat physical attributes, turn this specie ideal for testing the effects that Cd can have in the establishment of a halophytic specie independently of the type of marsh (Caçador et al., 2013). This species role as ecosystem sentinel of other estuarine contaminants in acute toxicity forms was already shown previously (Santos et al., 2014).

In the present work, the authors aimed to understand the effects of Cd acute toxicity on *J. acutus* seed germination, growth, photosynthetic apparatus as well as in photosynthetic pigments (including Cd substituted chlorophylls) and in the seedlings antioxidant response to acute metal stress for use as potential biomarkers in a sentinel specie. These experiments allow understanding the effect of this specific metal on the seedling germination and survival and its implications on cellular bioenergetics and redox homeostasis, while being potential candidates for biomarkers.

2. Materials and methods

2.1. Seed harvest and incubations

J. acutus seedlings were harvested in November 2011 in an undisturbed salt marsh of Tagus estuary within the old Expo 98' site. The inflorescences were collected, brought to the laboratory from which the seeds were extracted and kept in dry conditions. Seeds were incubated in ¼ Hoagland solution supplemented with $CdSO_4$ (Sigma–Aldrich Ultra-Pure) in order to make the desired Cd concentrations (0.05, 0.1, 0.5 and 1 μM). Approximately 20 seeds were placed in each petri dish with a Whatman GF/C. Each treatment (n = 3 petri dish, approx. 60 seeds) was soaked with 800 μL of the correspondent Cd concentration solution. The petri dishes were sealed with parafilm and placed in a FytoScope Chamber (Photon System Instruments, Czech Republic) in the dark at 25° C. Every three days the germinated seeds were counted until a maximum of 15 days. At the end of the experiment, the seedlings were collected and used for analysis. For all biochemical analysis was used 3 replicates composed by approximately 8–10 seedlings each one and were flash-frozen in liquid-N_2. Seedlings were also weighted and measured for total length. Germinations percentage was attained dividing the number of germinated seeds at each sampling moment by the total number of seeds in each petri dish. The germination index (GI) and rates (GR) were calculated according to AOSA (1983):

$$GI = \sum \frac{Number\ of\ germinated\ seeds}{Days\ since\ first\ count}$$

$$GR = \sum (Number\ germinated\ seeds \times Days\ since\ the\ first\ count)$$

2.2. Metal content analysis

Dry homogenized material (100 mg) was digested by adding 2 ml HNO3/HClO4 (7:1, v/v) in a reactor and heated at 110 °C for 6 h. After cooling overnight, the digestion products were filtered through Whatman No. 42 (2.5 μm of pore diameter) filters and diluted with distilled water to a total volume of 10 ml. Cadmium concentrations in the extracts were determined by atomic absorption spectrometry (Perkin–Elmer A Analyst 100). International certified reference materials (CRM 145, CRM 146 and BCR 62) were used to ensure accuracy and precision was determined by analyzing replicate samples. The concentrations in the reference materials determined by FAAS were not statistically different from their certified ones (t student; a = 0.05).

2.3. PAM fluorometry

Modulated chlorophyll fluorescence measurements were made in attached leaves in field with a FluoroPen FP100 PAM (Photo System Instruments, Czech Republic). All the measurements in the dark-adapted state were made after darkening of the leaves for at least 30 min. The minimal fluorescence (F_0) in dark-adapted state was measured by the measuring modulated light, which was sufficiently low (<0.1 μmol m^{-2} s^{-1}) not to induce any significant variation in fluorescence. The maximal fluorescence level (F_M) in dark-adapted state was measured by a 0.8 s saturating pulse at 8000 μmol m^{-2} s^{-1}. The maximum photochemical efficiency was assessed as $(F_M-F_0)/F_M$. The same parameters were also measured in light –adapted leaves, being F'_0 the minimum fluorescence, F'_M the maximum fluorescence and the operational photochemical efficiency. Rapid light curves (RLC) measurements, in dark-adapted leaves, were attained using the pre-programed LC1 protocol of the FluoroPen, consisting in a sequence of pulses from 0 to 500 μmol m^{-2} s^{-1}. During this protocol the F_0 and F_M as well as the maximum photochemical efficiency were measured. Each Φ_{PSII} measurement was used to calculate the electron transport rate (ETR) through photosystem II using the following equation: $ETR = \Phi_{PSII} \times PAR \times 0.5$, where PAR is the actinic photosynthetically active radiation generated by the FluoroPen and 0.5 assumes that the photons absorbed are equally partitioned between PSII and PSI (Genty et al., 1989). Without knowledge of the actual amount of light being absorbed, fluorescence measurements can only be used as an approximation for electron transport (Beer et al., 1998a,b and Runcie and Durako, 2004). Rapid light curves (RLC) were generated from the calculated ETRs and the irradiances applied during the rapid light curve steps. Each RLC was fitted to a double exponential decay function in order to quantify the characteristic parameters, alpha and ETR_{max} (Platt et al., 1980). The initial slope of the RLC (α) is a measure of the light harvesting efficiency of photosynthesis and the asymptote of the curve, the maximum rate of photosynthesis (ETR_{max}), is a measure of the capacity of the photosystems to utilize the absorbed light energy (Marshall et al., 2000). The onset of light

saturation (E_k) was calculated as the ratio between ETR_{max} and α. Excitation light of 650 nm (peak wavelength) from array of three light and emitting diodes is focused on the surface of the leaf to provide a homogenous illumination. The light intensity reaching the leaf was 3000 μmol m^{-2} s^{-1}, which was sufficient to generate maximal fluorescence in all individuals. The fluorescence signal is received by the sensor head during recording and is digitized in the control unit using a fast digital converter. The OJIP transient depicts the rate of reduction kinetics of various components of PS II. When dark-adapted leaf is illuminated with the saturating light intensity of 3500 μmol m^{-2} s^{-1} it exhibits a polyphasic rise in fluorescence (OJIP). Each letter reflects distinct inflection in the induction curve. The level O represents all the open reaction centres at the onset of illumination with no reduction of Q_A (fluorescence intensity lasts for 10 as). The rise of transient from O to J indicates the net photochemical reduction of Q_A (the stable primary electron acceptor of PS II) to Q_A^- (lasts for 2 ms). The phase from J to I was due to all reduced states of closed RCs such as Q_A^- Q_B^-, Q_A Q_B^{2-} and Q_A^- Q_B H_2 (lasts for 2–30 ms). The level P (300 ms) coincides with maximum concentration of Q_A^- Q_B^2 with plastoquinol pool maximally reduced. The phase P also reflects a balance between light incident at the PS II side and the rate of utilization of the chemical (potential) energy and the rate of heat dissipation (Zhu et al., 2005). From this analysis several photochemical parameters were attained (Table 1).

2.4. Gauss peak spectra pigment analysis

Seedlings for pigment analysis were freeze-dried in the dark during 48 h, after which they were grinded in pure acetone with a glass rod. To ensure complete disaggregation of the seed material, samples with acetone were subjected to a cold ultra-sound bath during 2 min. Extraction occurred at − 20 °C during 24 h in the dark to prevent pigment degradation. After extraction samples were centrifuged at 4000 rpm during 15 min at 4 °C. For pigment analysis it was employed the Gauss-Peak Spectra method (Küpper et al., 2007). Samples were scanned in a dual beam spectrophotometer from 350 nm to 750 nm at 0.5 nm steps. The absorbance spectrum was introduced in the GPS fitting library, using SigmaPlot Software. The employment of this library allowed to identify and quantify Chlorophyll a (MgChl a), Chlorophyll b (MgChl b), Cd-substituted Chlorophyll a (CdChl a), Cd-substituted Chlorophyll b (CdChl b), Pheophytin a (Pheo a), Antheraxanthin (Anthera), β-carotene, Lutein, Violoxanthin (Viola) and Zeaxanthin (Zea). In order to better evaluate the light harvesting and photo-protection mechanisms the De-Epoxidation State (DES) was calculated as:

$$DES = \frac{[Anthera] + [Zea]}{[Viola] + [Anthera] + [Zea]}$$

2.5. Anti-oxidant enzyme assays

All enzymatic analyses were performed at 4 °C. Briefly, it was used a proportion of 500 mg of fresh biomassfor 8 ml of 50 mM sodium phosphate buffer (pH 7.6) with 0.1 mM Na-EDTA, for extraction. Due to the low biomass of each seedling, each replicate was composed by 8–10 seedlings pooled together. The homogenate was centrifuged at 8923 rpm for 20 min, at 4 °C, and the supernatant was used for the enzymatic assays. Catalase activity was measured according to the method of Teranishi et al. (1974), by monitoring the consumption of H_2O_2, and consequent decrease in absorbance at 240 nm. ($\varepsilon = 39.4$ mM^{-1} cm^{-1}). The reaction mixture contained 50 mM of sodium phosphate buffer (pH 7.6), 0.1 mM of Na-EDTA, and 100 mM of H_2O_2. The reaction was started with the addition of the extract. Ascorbate peroxidase was assayed according to Tiryakioglu et al. (2006). The reaction mixture contained 50 mM of sodium phosphate buffer (pH 7.0), 12 mM of H_2O_2, 0.25 mM L-ascorbate. The reaction was initiated with the addition of 100 μL of enzyme extract. The activity was recorded as the decrease in absorbance at 290 nm and the amount of ascorbate oxidized was calculated from the molar extinction coefficient of 2.8 mM^{-1} cm^{-1}. Guaiacol peroxidase was measured by the method of Bergmeyer et al. (1974) with a reaction mixture consisting of 50 mM of sodium phosphate buffer (pH 7.0), 2 mM of H_2O_2, and 20 mM of guaiacol. The reaction was initiated with the addition of 100 μL of enzyme extract. The enzymatic activity was measured by monitoring the increase in absorbance at 470 nm ($\varepsilon = 26.6$ mM^{-1} cm^{-1}). Superoxide dismutase activity was assayed according to Marklund and Marklund (1974) by monitoring the reduction of pyrogallol at 325 nm. The reaction mixture contained

Table 1
Summary of Fluorometric analysis parameters and their description.

Photosystem II efficiency	
F'_0 and F_0	Basal Fluorescence under weak actinic light in light and dark adapted leaves.
F'_M and F_M	Maximum Fluorescence measured after a saturating pulse in light and dark adapted leaves.
F'_v and F_v	Variable fluorescence light ($F'_M - F'_0$) and dark ($F_M - F_0$) adapted leaves.
PSII operational and maximum quantum yield	Light and dark adapted Quantum yield of primary photochemistry, equal to the efficiency by which an absorbed photon trapped by the PSII reaction centre will result in reduction of Q_A–Q^-_A.
Rapid light curves (RLCs)	
rETR	Relative electron transport rate at each light intensity (rETR = QY × PAR × 0.5) (Genty et al., 1989).
α	Photosynthetic efficiency, obtained from the initial slope of the RLC (Marshall et al., 2000).
OJIP derived parameters (Strasser and Stribet, 2001)	
ψ_{P0}	Maximum Yield of Primary Photochemistry.
ψ_{E0}	Probability that an absorbed photon will move an electron into the ETC.
ψ_{D0}	Quantum yield of the non-photochemical reactions.
φ_0	Probability of a PSII trapped electron to be transported from Q_A to Q_B.
RC/ABS	Fraction of active QA-reducing, PS II reaction centres per light absorbed by PSII and which corresponds to the reaction centre II density within the antenna chlorophyll bed of PSII.
Diving force for photosynthesis (DF_{ABS})	$DF_{ABS} = DF_{RC} + DF\psi_{P0} + DF\varphi$)
Driving force for trapping electronic energy ($DF\psi_{P0}$)	$DF\psi_0 = \log(\psi_{P0}/(1 - \psi_{P0})$
Driving force for electron transport ($DF\varphi$)	$DF\varphi = \log(\varphi_0/(1 - \varphi_0)$
Driving force for energy absorption (DF_{RC})	$DF_{RC} = \log$ (RC/ABS)

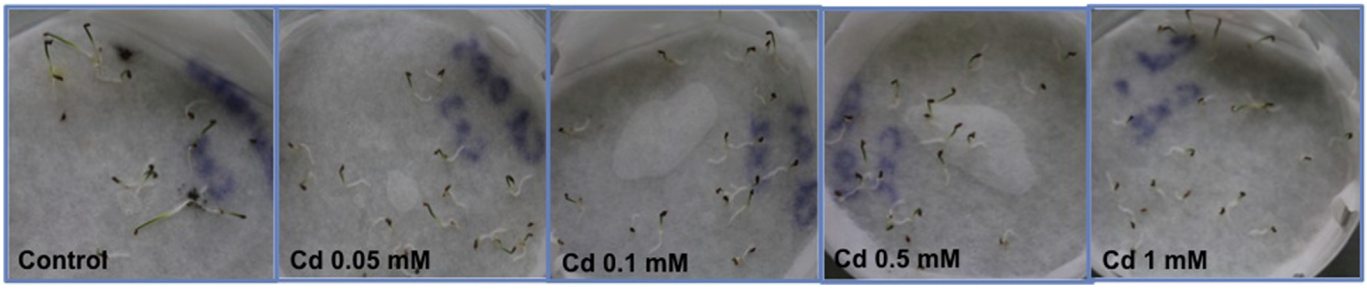

Fig. 1. *J. acutus* seedlings response to increasing cadmium treatments.

50 mM of sodium phosphate buffer (pH 7.6), 0.1 mM of Na-EDTA, 3 mM of pyrogallol, Mili-Q water. The reaction was started with the addition of 10 μL of enzyme extract. Control assays were done in the absence of substrate in order to evaluate the auto-oxidation of the substrates.

2.6. Statistical analysis

Due to the lack of homogeneity and normality of the data, the statistical significance between the results obtained among treatments was tested using Krustal-Wallis non-parametric test using Statistica Software 10 (StataSoft Inc.). Spearman correlations were applied in order to evaluate the existence of direct effects between the metal concentrations and the biological variables.

3. Results

3.1. Seed germination

After 15 days at dim light (less than 20 μmol photons m^{-2} s^{-1}) in the presence of various cadmium treatments almost all seeds had germinated (Fig. 1). The first germination signs could be detected at

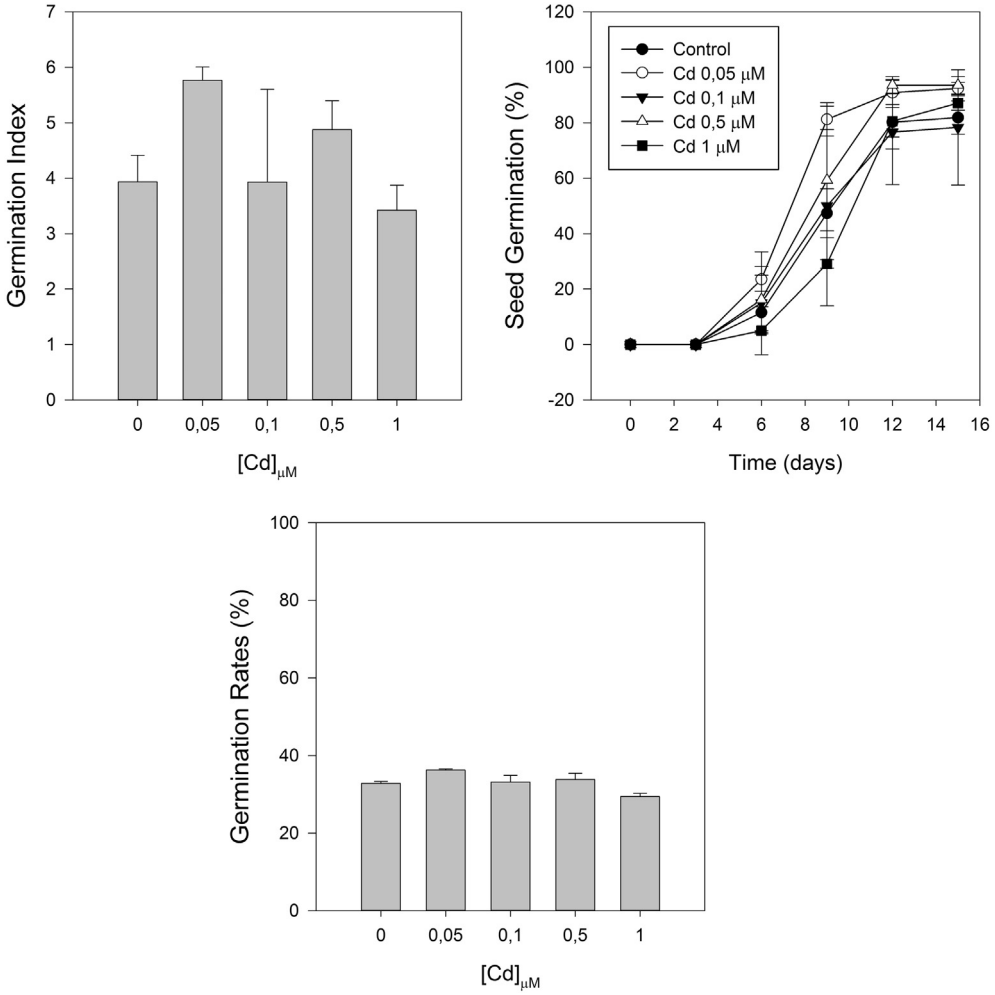

Fig. 2. Germination index, Seed germination and germination rates of *J. acutus* seedlings with increasing cadmium treatments (average ± standard deviation, n = 3. Letters indicate significant differences at $p < 0.05$).

the 6th of experience (as shown in Fig. 2) and its percentage increased until day 12. As can be observed, the highest percentage of germination was at 0.05 and 0.5 μM Cd treatments, reaching almost 100%, being higher than control. Concerning the germination rates, there was a maximum at 0.05 μM Cd and the lowest was at 1 μM. In relation to germination indexes, the higher value was achieved upon application of 0.05 μM Cd and the minimum at 1 μM, as can be observed in Fig. 2.

3.2. Biomass measurements and Cd tissue concentration

Regarding the seedlings length measurement, was higher in all Cd treatments relatively to the control, being the highest value verified at the treatment of 0.1 μM of Cd. On the other hand, biomass presented the opposite pattern, being the control where can be found the highest value of fresh weight. Given this, as expected the ratio between fresh weight and length was higher in the control, as is shown in Fig. 3. Relatively to the metal content, the seedlings showed higher metal concentrations with the increasing cadmium treatments. Metal concentration in the seedlings was higher at the highest cadmium treatment (1 μM) and the lowest metal concentration found in seedlings was in the control. The internal Cd concentration of the seedlings rose with the applied Cd doses, being this way dose-dependent, as shown by Fig. 4.

3.3. PSII quantum efficiencies and variable fluorescence

In respect to maximum PSII quantum efficiencies (dark-adapted seedlings) there was difference among cadmium treatments. Concerning the operational PSII quantum efficiencies (light-adapted seedlings) although being lower than in dark-adapted there wasn't also any significant fluctuations, as shown in Fig. 5.

Regarding the variable fluorescence, both dark and light-adapted seedlings, had a maximum at the highest Cd concentration (1 μM). However in light adapted seedlings the variable fluorescence increased along with the increasing gradient of Cd doses applied.

Regarding both rETR at different light intensities and maximum rETR, higher values at control and 0.5 μM of Cd and a minimum at 1 μM of Cd could be observed. Also, the photosynthetic rate (α),

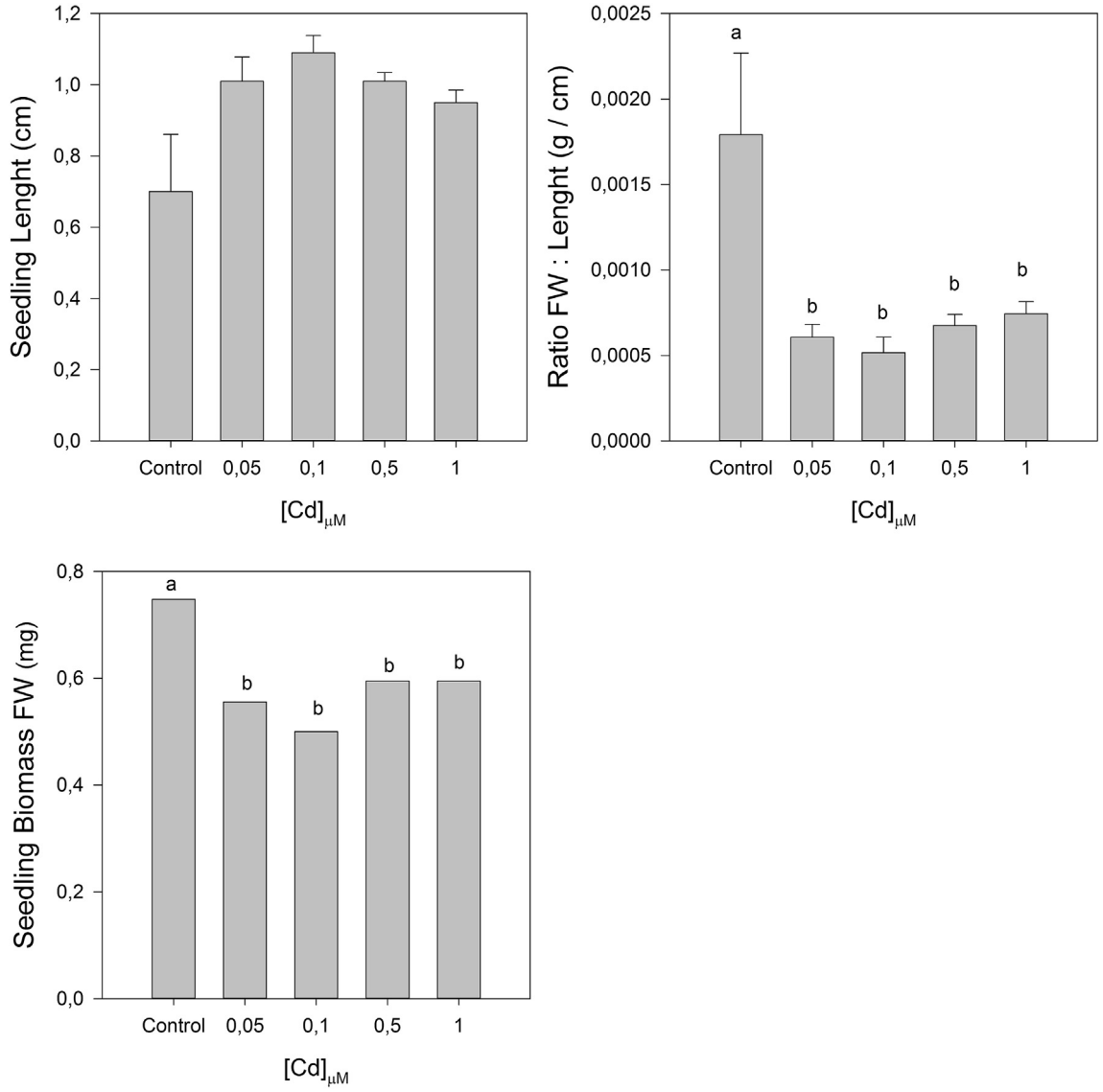

Fig. 3. Growth and Fresh Biomass of seedlings from *J. acutus*, exposed to increasing cadmium treatments (average ± standard deviation, n = 3. Letters indicate significant differences at $p < 0.05$).

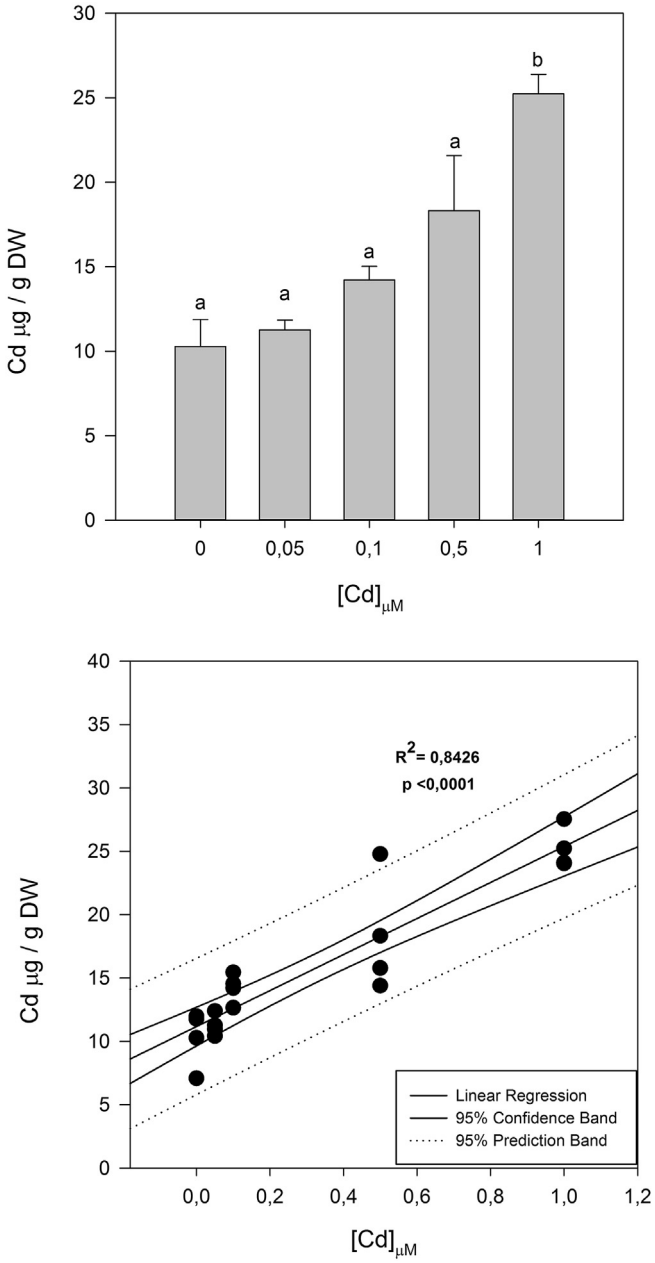

Fig. 4. Cadmium accumulation in tissues of *J. acutus* (average ± standard deviation, n = 3. Letters indicate significant differences at $p < 0.05$).

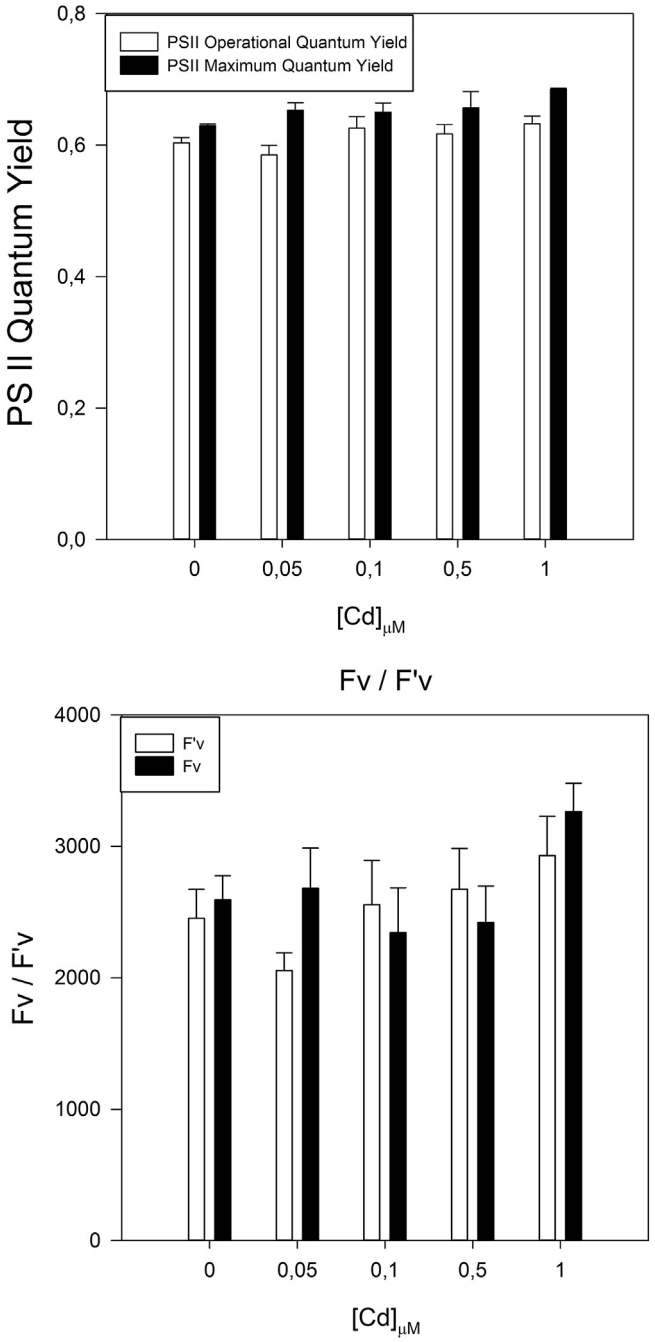

Fig. 5. Operational and maximum PS II quantum yield of seedlings and variable fluorescence with different cadmium concentrations (average ± standard deviation, n = 3. Letters indicate significant differences at $p < 0.05$).

given by the initial slope of the rETR vs light curves, had its maximum at the same Cd concentrations (0.5 and 1 µM) but its minimum was at observed at of the Cd treatment of 0.1 µM. As for the onset of light absorption (E_k), all the Cd treatments presented higher values in comparison to the control, reaching a maximum at 0.05 µM and a minimum at 0.5 µM of Cd as could be seen in Fig. 6.

3.4. Pigment concentrations

Overlooking the pigments concentration in Table 2, it is possible to observe a reduction of the MgChl a and b with the increasing concentrations of Cd, with the lowest value found at the 1 µM Cd treatment for both chlorophylls. Concerning the ratio between Chl a and b, the highest value was verified in the control, decreased with the increasing Cd treatments, aside of being similar among Cd treatments (Fig. 7).

In relation to carotenoids, also shown in Table 2, violaxanthin showed a marked decrease with the increasing concentration of Cd. The remaining carotenoids measured, showed an increase in concentration, with the highest value at 0.05 µM of Cd for Antheraxantin and 0.1 µM for β−carotene as well as Lutein and Zeaxanthin. Given this, and the decline in Mg-chlorophylls, the ratio between total carotenoids to Mg-chlorophylls was higher with the increasing dose of Cd concentration, as shown in Fig. 7, being indicative of a stress condition of the seedlings. Chlorophyll Degradation Index (CDI) and the De-epoxidation state (DES) presented a decrease with increasing doses of Cd, with both reaching a minimum at 0.1 µM of Cd.

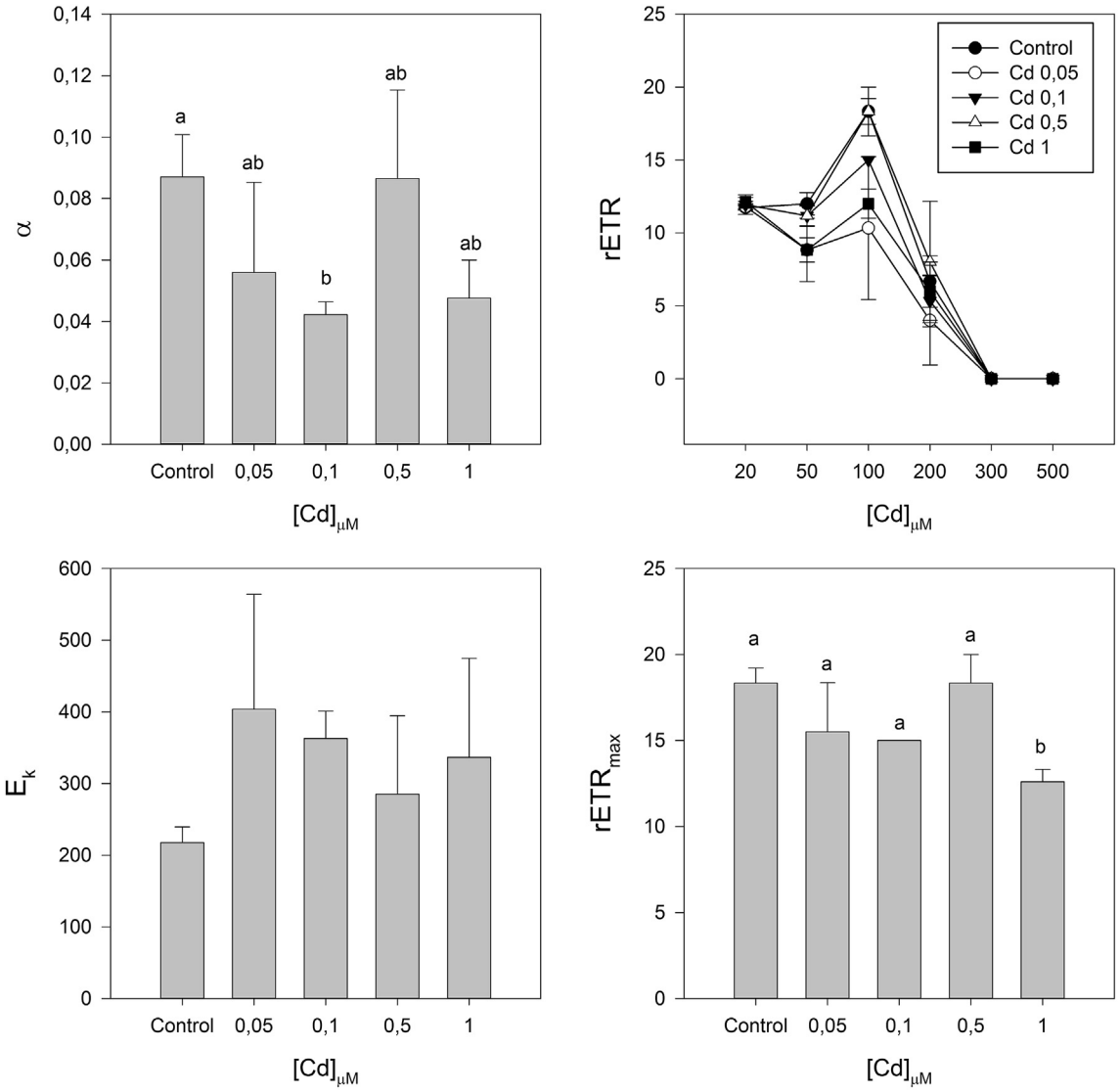

Fig. 6. Relative electron transport rate (rETR) at different light intensities, maximum electron transport rate ($rETR_{max}$), photosynthetic rate (α) and onset of light saturation (Ek) of seedlings, with increasing concentrations of cadmium (average ± standard deviation, n = 3. Letters indicate significant differences at $p < 0.05$).

Table 2
Pigment (chlorophylls and degradation products and carotenoids) concentration (μg/g FW) in *J. acutus* individuals exposed to different levels of Cd (average ± standard deviation, n = 3. Letters indicate significant differences at $p < 0.05$).

[Cd] mM	MgChl a	MgChl b	Pheo A	Antheraxanthin	β−carotene	Lutein	Violoxanthin	Zeaxanthin
0	339.8 ± 38.4a	129.1 ± 15.4	8.8 ± 2.1^{a}	$7.0 \times 10^{-8} \pm 7.0 \times 10^{-8a}$	11.2 ± 1.47^{a}	24.6 ± 2.3	24.9 ± 2.1^{a}	11.9 ± 1.6^{a}
0.05	229.4 ± 8.9^{b}	139.7 ± 5.9	114.6 ± 3.1^{b}	17.6 ± 0.9^{b}	35.0 ± 1.3^{b}	20.6 ± 1.1	6.7 ± 0.9^{b}	44.2 ± 1.3^{b}
0.1	267.2 ± 43.6^{b}	165.2 ± 27.9	137.9 ± 22.7^{b}	16.9 ± 1.9^{b}	42.4 ± 5.5^{b}	21.8 ± 1.9	2.9 ± 2.0^{b}	46.8 ± 5.5^{b}
0.5	218.5 ± 2.8^{b}	134.9 ± 3.3	109.5 ± 7.7^{b}	14.0 ± 1.3^{b}	32.2 ± 2.0^{b}	17.1 ± 1.3	3.3 ± 0.8^{b}	39.2 ± 3.0^{b}
1	210.5 ± 9.5^{b}	128.1 ± 3.5	112.4 ± 8.3^{b}	16.9 ± 1.86^{b}	33.2 ± 1.2^{b}	20.4 ± 1.6	6.8 ± 2.3^{b}	42.9 ± 2.8^{b}

Regarding the substituted chlorophylls, the highest value found in CdChl a and b was at 0.05 μM cadmium treatment, contrasting with the lower concentration at the control treatment. However CdChl b showed dose−response pattern between 0.1 and 1 μM (increasing with the increasing dose of exogenous Cd applied), despite the fact that Chl concentration was below the highest value verified as can be observed in Fig. 8.

3.5. Kautsky curves and transient OJIP parameters

Relatively to the chlorophyll transients, all the treatments showed an identical photochemical phase, corresponding to O-J phase. The differences between treatments were more evident in the thermal phase (J-I-P), as shown by Fig. 9. As can be seen, the increase in the thermal phase was higher upon the application of 0.1 μM of Cd, being even slightly above the control. On the other hand, the treatment with highest concentration of Cd was the one that led to the lower thermal phase among all treatments.

Regarding the driving forces variation, a major decrease was found in the driving force for photosynthesis (DF_{ABS}). This marked decrease was mainly due to the decline in the driving force for excitation energy trapping ($DF\psi$) and for the conversion of

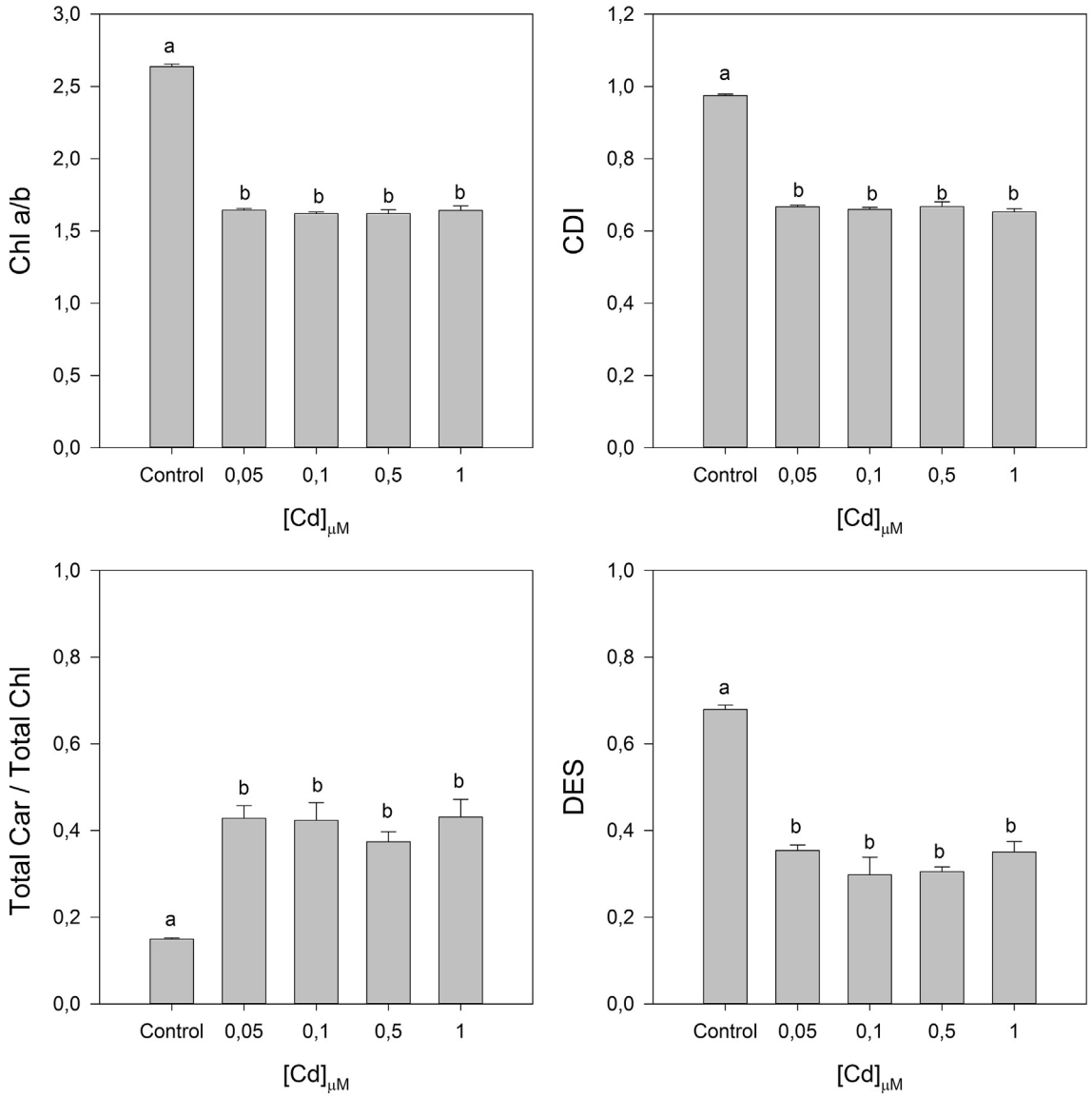

Fig. 7. Pigments ratio in seedlings exposed to different cadmium concentrations (average ± standard deviation, n = 3. Letters indicate significant differences at $p < 0.05$).

excitation energy to electron transport (DF_{φ}), although with a minor influence. On the other hand, the driving force for light energy absorption (DF_{RC}) was not affected by the different concentrations of Cd, being constant among treatments, as shown by Fig. 10.

3.6. Antioxidant enzymatic activities

Observing the data about antioxidant enzymes, the only enzyme that didn't show any activity was CAT (data not shown). SOD activity was highest on the last Cd treatment (1 μM), contrasting with the lowest value of activity at the treatment of 0.05 μM of Cd. GPx showed a similar activity in all treatments, except in the individuals exposed to 0.1 μM of Cd, where no activity was registered, as shown by Fig. 11. Relatively to APx activity, it increased along with cadmium gradient, with the highest value of activity observed in the seedlings grown with 1 μM Cd.

3.7. Acute Cd metabolic interferences

Using a correlation matrix (Table 3) it was possible to assess which biomarkers are more correlated with the Cd-dose applied and with the effective Cd concentration within the plant tissues. Several of the evaluated parameters presented good correlations, not only with the endogenous Cd concentrations but also with the exogenous Cd concentration applied. While in most cases Cd application lead to a decrease in the evaluated parameters, PSII Maximum Quantum Yield and the APx activity showed an evident positive feedback to Cd stress. Most of the parameters showed a negative feedback to Cd application with exception of one counteractive measure proxy, APx activity, in accordance to the abovementioned results.

4. Discussion

The bioprospection of plant species that could be used as biotools for managing heavy metal pollution, especially in acute situations such as severe uncontrolled discharges, is one of the fundamental guidelines for designing and developing of effective methodologies for environmental monitoring. Nevertheless and with equally high importance arises the need to evaluate how potentially hyperaccumulator species behave and tolerate acute

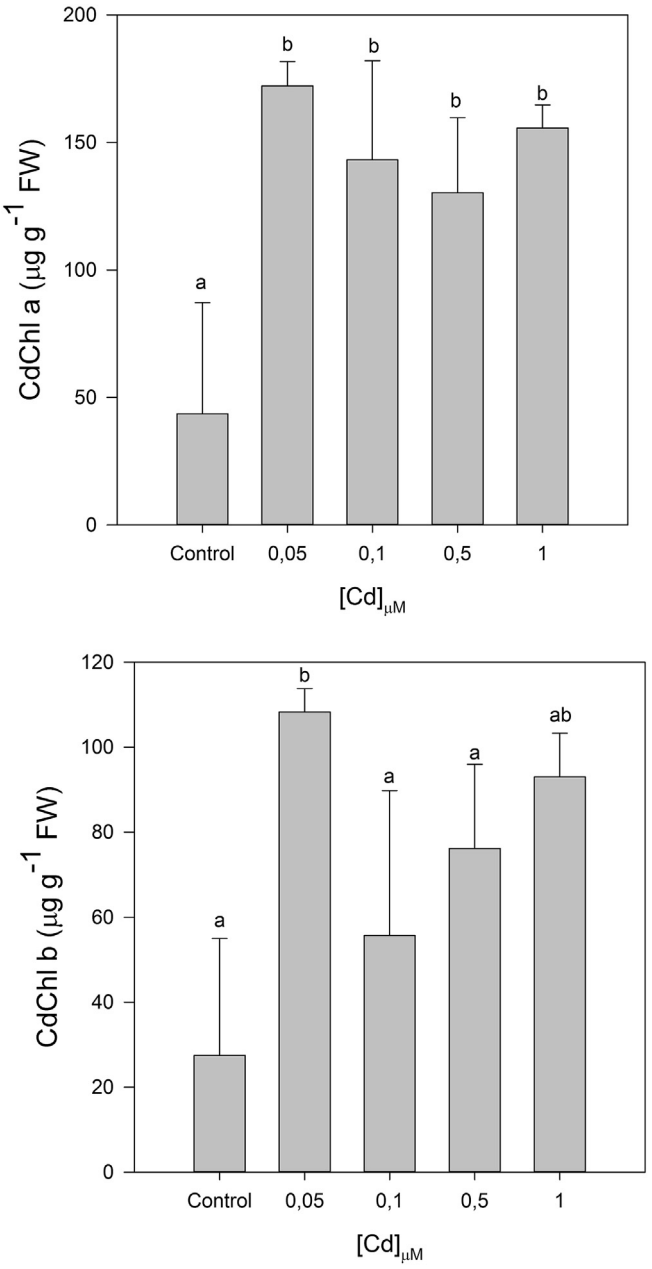

Fig. 8. Cd-Chl a and b concentration in seedlings, treated with increasing cadmium treatments (average ± standard deviation, n = 3. Letters indicate significant differences at $p < 0.05$).

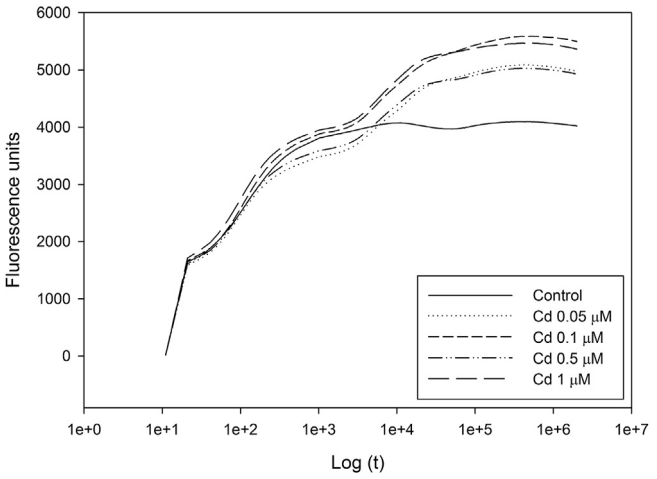

Fig. 9. Chlorophyll a fluorescence transients O-J-I-P in control and with increasing cadmium concentrations of *J. acutus* seedlings (average ± standard deviation, n = 3. Letters indicate significant differences at $p < 0.05$).

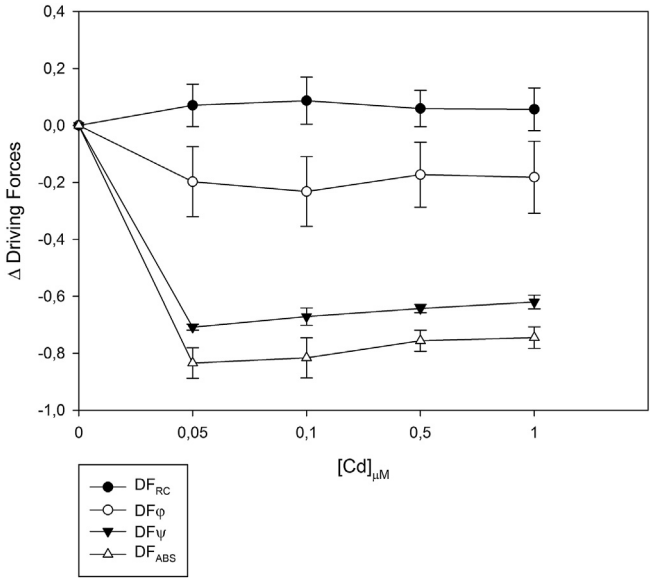

Fig. 10. Variation of Driving Forces in *J. acutus* seedlings where DF_{RC} is the driving force for light energy absorption, DF_{ϕ} is the driving force for excitation energy to electron transportation, DF_{ψ} is the driving force for trapping of excitation energy and DF_{ABS} is the driving force for photosynthesis (average ± standard deviation, n = 3. Letters indicate significant differences at $p < 0.05$).

metal stress and more importantly how it impacts their primary productivity. Stress factors are lesser effective in seed stage than in the following phases after starting the development of vegetative processes and consequently becoming more susceptible of being affected by stressors (Li et al., 2005). In the present study, it was found that the lower Cd concentration (0.05 µM) enhanced seed germination, since the percentage of seeds germinated was higher (approximately 90%) than in control (around 80%). According to Mel'nichuck (1990), seed germination can be promoted by Cd^{2+} at low concentrations, around 10^{-5} µM. Moreover, Zhang et al. (2012), obtained higher germination rate and index, as well as higher values for shoot length, root length and dry biomass when exposed *Elymus dahuricus* seedlings to Cd treatments. On the other hand, germination inhibition can also occur due Cd^{2+} exposure. For example, Prodanovic et al. (2012) showed inhibition rates around 80% in seeds of Serbian spruce (*Picea omorika*) with 1 µM of Cd^{2+}; also, Zhang et al. (2010) registered inhibition at low concentration as 0.2 µM in *Achnatherum inebrans*. In *Suaeda salsa*, Liu et al. (2012) had only 10% of seeds germinated after treatment with 0.05 µM of Cd, which was similar to the lower concentration used in the present study. These facts suggest that seeds of *J. acutus* could have a higher resistance to Cd-driven stress, than other studied species. The seedlings in this study experienced a growth inhibition, after Cd treatments above 0.1 µM. Similar results were obtained by Liu et al. (2012) where higher doses of cadmium lead to growth inhibition. Ghnaya et al. (2005) also had at some degree a decrease in growth of *Sesuvium portulacastrum* and *Mesembryanthenum crystallum*. These authors suggested that this impairment in growth could be due to a disturbance in the plant nutrition, since Cd could interfere in the Ca and K uptake. Along with this, a decline in the biomass was observed. This fresh biomass reduction could be due

to the water loss, caused by the membrane damage due to Cd-induced stress at excessive concentrations (Najeeb et al. 2011).

Mg-chlorophyll a and b also showed a decrease in their concentration. This decline in the Mg-chlorophyll content can be due to the presence of Cd, leading ultimately to chlorosis (Baszyńki et al., 1980). Also, De Filippis et al. (1981) indicated that Cd, Zn and Hg could interfere with the chlorophyll biosynthesis. Alongside with this decline in the chlorophyll content, the Chlorophyll Degradation Index (CDI) also showed a decrease indicating that this reduction wasn't due to chlorophyll degradation into pheophythin. Another parameter that supports this fact was the increase in the Cd-chlorophylls. This suggests, that the main reason of chlorophyll (MgChl a) decrease was due to the substitution of Mg^{2+} by Cd. Krupa (1988) and Krupa et al. (1987) also showed that Cd decreased the ratio of trimeric/monomeric LHC II in radish, due to disturbed pigment binding. Küpper et al. (1996) also suggests that these Cd-substituted chlorophyll is highly unstable, and thus decreases the efficiency of the LHC II.

Although the fact that Cd^{2+} can cause the arresting of chlorophyll synthesis, plastoquinone and carotenoids, it also restricts the PS II related electron transport, due to structural and functional changes in tylakoid membranes, reduced activity of ferrodoxin $NADP^{+}$ oxireductase and arrested plastoquinone synthesis (Baszyńki et al., 1980; Barceló et al., 1988; Krupa and Baszynski, 1995). This obstruction of electron transport happens due to the substitution of Mg^{2+} by Cd^{2+} on the chlorophyll molecule, making it less efficient (Kalaji and Loboda, 2007). This inefficiency can lead to an accumulation of excessive energy that has to be dissipated to prevent serious damages to the plant. One of the most efficient mechanisms of energy dissipation is the conversion of violaxanthin to zeaxanthin, through the xanthophyll cycle (Demmig-Adams and Adams, 1992; Reinhold et al., 2008). In this study the seedlings, did lose some of the excessive energy created by the impairment of PS II function, throughout this pathway. Supporting this, all treatments with Cd showed an increase in the DES value and Zeaxanthin concentrations also rose, as can be observed on Fig. 7 and Table 2, respectively. Other possible pathway to counteract the excessive energy accumulation is through heat dissipation (Duarte et al., 2013a). Looking for fluorescence transient O-J-I-P, its shows that there was an increase in the thermal phase (J-I-P) in all cadmium

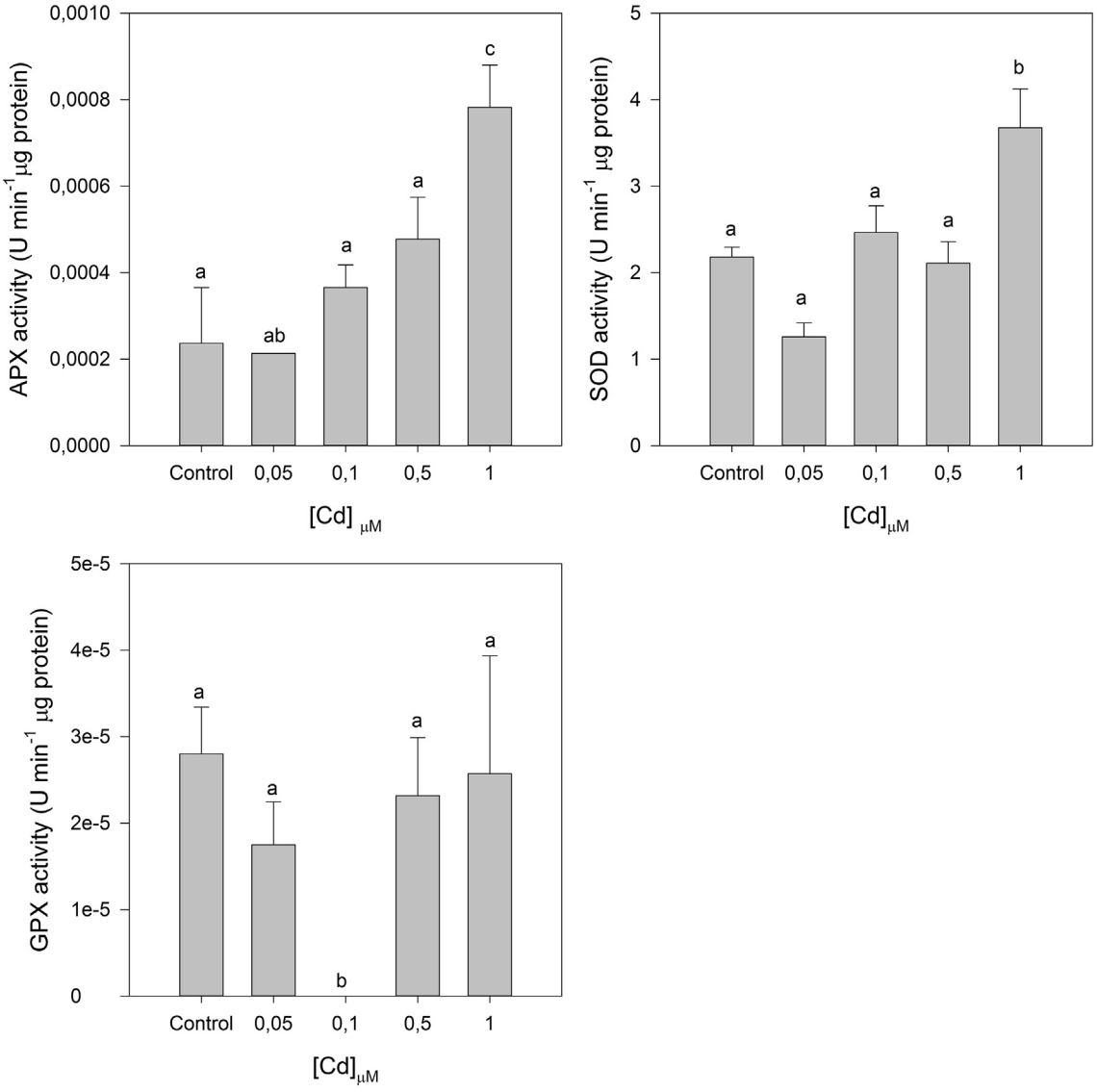

Fig. 11. Ascorbate peroxidase (APx), Superoxide Dismutase and Guaiacol peroxidase (GPx) in *J. acutus* seedlings, with different cadmium treatments (average ± standard deviation, n = 3. Letters indicate significant differences at $p < 0.05$).

Table 3
Correlation coefficients (r^2) between the analyzed parameters and the verified Cd concentrations in the seedlings tissues (μg g DW^{-1}) and the applied exogenous Cd concentration (*p < 0.05; **p < 0.01; ***p < 0.001; n.d., non-defined).

Parameter	Cd (μg g DW^{-1})	Exogenous Cd (μM)
Germination index	−0.40	−0.27
Germination rate	−0.50	−0.49
Seedling biomass	−0.37	−0.40
Seedlinglength	−0.02	−0.04
Biomass/length ratio	−0.38	−0.40
F'v	0.44	0.44
PSII operational quantum yield	0.43	0.51
Fv	0.34	0.39
PSII maximum quantum yield	0.63*	0.61*
Photosynthetic efficiency (a)	0.15	−0.14
Maximum ETR	−0.01	−0.31
Onset light saturation (Ek)	0.00	0.10
DF_{RC}	−0.18	−0.24
DF_{φ}	0.17	0.15
$DF\psi$	−0.71**	−0.76**
DF_{ABS}	−0.53*	−0.60*
MgChl a	−0.57	−0.70**
MgChl b	−0.13	−0.08
Pheo A	0.25	0.38
Antheraxanthin	0.12	0.34
β carotene	0.16	0.34
Violaxanthin	−0.52*	−0.56*
Zeaxanthin	0.10	0.35
De-epoxidation state (DES)	−0.53*	−0.56*
Chl a/b raio	−0.29	−0.51
Total car/cotal Chl	0.32	0.48
Chl degradation index	−0.45	−0.63*
CdChl a	0.08	0.26
CdChl b	0.10	0.23
CAT activity	n.d.	n.d.
APx activity	0.69**	0.78***
GPx activity	−0.03	0.02
SOD activity	0.53*	0.55*

treatments, concomitant with the seedling lack of efficiently using the energy harvested, and thus dissipating it through heat. Supporting this, also the variable fluorescence was higher with Cd treatments, indicating a photochemical stress condition. Related to this is the loss of photosynthetic capacity, reflected in the photochemical driving forces. First of all, there was a decrease in the driving force for light energy absorption (DF_{RC}) above 0.1 μM Cd treatment. Along with this, an increase in DFϕ occurred (driving force involved in the excitation energy for electron transportation) indicating an inefficiently usage of the harvested energy (Eullaffroy et al. 2009). However, the driving force for photosynthesis (DF_{ABS}) was mostly influenced by the decrease in driving force for trapping of excitation energy (DF_{ψ}). In addition, some ultra structure disorganization in the chloroplast, e.g. disappearance of grana or development of plastoglobuli could be consequence of Cd and Pb in higher plants as well as others heavy metals do in algae (Rebechini and Hanzely, 1974; Lindsey and Lineberger, 1981; Thomas et al. 1980), can also be in the basis of this lost of efficiency.

Reactive Oxygen Species (ROS) can be produced as a direct consequence of heavy metal exposure or indirectly by excessive energy accumulation, causing in both cases cellular damage. To counteract or diminish the extent of the damage caused by these reactive species, cells have antioxidant mechanisms suited for protection. These mechanisms are constituted by enzymatic systems such superoxide dismutase (SOD), Ascorbate peroxidase (APx), guaiacol peroxidase (GPx) and non-enzymatic systems such as ascorbic acid, thiols, cysteine, phenolics and flavonoids (Halliwell and Gutteridge, 1993). SOD appears as a first line of defense, converting superoxide radicals into H_2O_2. In this study SOD activity showed a positive trend with increasing Cd treatments. This increasing activity that was observed could be due to an augmented cellular concentration of superoxide radicals generated by Cd oxidative damage, or due to a direct effect on SOD coding genes, inhibiting its synthesis (Chongpraditnum et al. 1992). In fact, Cd can promote the activity of some enzymes as well, whether by direct effector through interference in enzyme synthesis or immobilization of their inhibitors. (Blinda et al. 1997; Van Assche and Clijsters, 1990; Przymusiński et al., 1995; Chen and Kao, 1995; Stroiński, 1999). Although SOD is crucial for ROS detoxification, its activity is also responsible for the production of hydrogen peroxide. This product can also cause damage in several cellular components (such as lipids, DNA, ribosomes) and to counteract these effects there are some specific peroxidases that are normally involved in Cd-driven ROS detoxification (Duarte et al., 2013b). Higher SOD activities lead inevitably to high H_2O_2 production as reaction product, and thus was expected that APx should be stimulated increasing its activity. In fact this enzyme proved to have a very good dose–response correlation, as was already detected in previous studies (Santos et al., 2014). GPx also showed an increase with higher activities of SOD, although no activity was registered in 0.1 μM Cd treatments. Oppositely, CAT didn't show any activity along Cd treatments. This Cd^{2+} CAT-inhibition is mostly due their interactions with enzyme SH-groups. SH-groups are essential to enzyme reaction centre and to the stabilization of enzyme tertiary structure. Ultimately, Cd^{2+} will interfere with enzyme conformation (Levina, 1972). This could help to explain the fact that, in this study, CAT didn't show any activity. However the same was not observed by Liu et al. (2012), where this enzyme showed a linear response to the increase of Cd treatments.

5. Conclusions

Bioprospection of potential heavy metal hyperaccumulators focuses not only the phytoremediative ability of the specie towards a specific metal while producing high amounts of biomass, but should also focus in the health status of the plant as well as possible causes and counter-measures of stress. This last approach can also provide to be a source of important biomarkers of acute toxicity for biomonitoring proposes. Seedling growth suffered a decline as well as biomass, with increasing Cd treatments. The presence of Cd in tissues was dependent of the metal concentration in the culture medium, since its concentration in the plant biomass was increasingly higher with increasing cadmium treatments, showing a typical dose–response pattern. Seedlings also showed an augment in Cd-substituted chlorophylls, which is in the basis of their loss in photosynthetic efficiency, coupled with an increase in the energy dissipation both by heat and fluorescence. Also Cd excessive concentrations induced oxidative stress, which explain the increase in antioxidant enzymes activities, with SOD enzyme showing the highest activity among all the enzymes tested, with a clear dose-related pattern. This enzyme along with the concentration of Cd-Chl, appears as efficient biomarkers of Cd toxicity in *J. acutus*. Despite these important mechanism network, some isolated parameters here presented appear to provide efficient biomarkers of Zn acute toxicity as powerful tools for biomonitoring in Cd-contaminated environments.

Acknowledgments

The authors would like to thank to the “Fundação para a Ciência e Tecnologia (FCT)” for funding the research in the Marine and Environmental Sciences Centre (MARE) throughout the project UID/MAR/04292/2013 and this specific work throughout the ECOSAM project (PTDC/AAC-CLI/104085/2008). B. Duarte investigation was supported by FCT throughout a PhD grant (SFRH/BD/75951/2011).

References

Assche, F.V., Clijsters, H., 1990. Effects of metals on enzyme activity in plants. Plant Cell Environ. 13 (3), 195–206.

Association of Official Seed Analysis (AOSA), 1983. Seed Vigor Testing HandBook. Contribution N°32 to the Handbook on Seed Testing.

Barceló, J., Vásquez, M.D., Poschenrieder, Ch, 1988. Structural and ultrastructural disorders in cadmium-treated bush bean plants (*Phaseolus vulgaris* L.). New Phytol. 108 (1), 37–49.

Baszyński, T., Wajda, L., Król, M., Wolińska, D., Krupa, Z., Tukendorf, A., 1980. Photosynthetic activities of cadmium-treated tomato plants. Physiol. Plant. 48, 365–370.

Beer, S., Ilan, M., Eshel, A., Weil, A., Brickner, I., 1998a. The use of pulse amplitude modulated (PAM) fluorometry for in situ measurements of photosynthesis in two red sea faviid corals. Mar. Biol. 131, 607–612.

Beer, S., Vilenkin, B., Weil, A., Veste, M., Susel, L., Eshel, A., 1998b. Measuring photosynthesis in seagrasses by pulse amplitude modulated (PAM) fluorometry. Mar. Ecol. Prog. (Series 174), 293–300.

Bergmeyer, H.U., Gawehn, K., Grassl, M., 1974. Enzymes as biochemical reagents. In: Bergmeyer, H.U. (Ed.), Methods in Enzymatic Analysis. Academic Press, New York.

Blinda, A., Koch, B., Ramanjulu, S., Dietz, K., 1997. De novo synthesis and accumulation of apoplastic proteins in leaves of heavy metal-exposed barley seedlings. Plant Cell Environ. 20 (8), 969–981.

Caçador, I., Vale, C., Catarino, F., 1996. The influence of plants on concentration and fractionation of Zn, Pb, and Cu in salt marsh sediments (Tagus Estuary, Portugal). J. Aquat. Ecosys. Health 5, 193–198.

Caçador, I., Costa, J.L., Duarte, B., Silva, G., Medeiros, J.P., Azeda, C., Castro, N., Freitas, J., Cabral, H., Costa, M.J., 2012. Macroinvertebrates and fishes as biomonitors of heavy metal concentration in the Seixal Bay (Tagus estuary): which species perform better? Ecol. Indic. 19, 184–190.

Caçador, I., Neto, J.M., Duarte, B., Barroso, D.V., Pinto, M., Marques, J.C., 2013. Development of an angiosperm quality assessment index (AQuA – index) for ecological quality evaluation of Portuguese water bodies – a multi-metric approach. Ecol. Indic. 25, 141–148.

Chen, S.L., Kao, C.H., 1995. Cd induced changes in proline level and peroxidase activity in roots of rice seedlings. Plant Growth Regul. 17 (1), 67–71.

Chongpraditnum, P., Mori, S., Chino, M., 1992. Excess cover induces a cytosolic Cu, Zn-superoxide dismutase in soybean root. Plant Cell Physiol. 33, 239–244.

De Filippis, L.F., Hampp, R., Ziegler, H., 1981. The effects of sublethal concentrations of zinc, cadmium and mercury on Euglena. Archives Microbiol. 128 (4), 407–411.

Demmig-Adams, B., Adams II, W.W., 1992. Photoprotection and other responses of plants to light stress. Annu. Rev. Plant Physiol. Plant Mol. Biol. 43, 599–626.

Duarte, B., Reboreda, R., Caçador, I., 2008. Seasonal variation of extracellular enzymatic activity (EEA) and its influence on metal speciation in a polluted salt marsh. Chemosphere 73, 1056–1063.

Duarte, B., Caetano, M., Almeida, P., Vale, C., Caçador, I., 2010. Accumulation and biological cycling of heavy metal in the root-sediment system of four salt marsh species, from Tagus estuary (Portugal). Environ. Pollut. 158, 1661–1668.

Duarte, B., Caçador, I., 2012. Particulate metal distribution in Tagus Estuary (Portugal), during a flood episode. Mar. Pollut. Bull. 64, 2109–2116.

Duarte, B., Couto, T., Freitas, J., Valentim, J., Silva, H., Marques, J.C., Caçador, I., 2013. Abiotic modulation of *Spartina maritima* photosynthetic ecotypic variations in different latitudinal populations. Estuar. Coast. Shelf Sci. 130, 127–137.

Duarte, B., Santos, D., Caçador, I., 2013. Halophyte anti-oxidant feedback seasonality in two salt marshes with different degrees of metal contamination: search for an efficient biomarker. Funct. Plant Biol. 40, 922–930.

Eullaffroy, P., Frankart, C., Aziz, A., Couderchet, M., Blaise, C., 2009. Energy fluxes and driving forces for photosynthesis in *Lemna minor* exposed to herbicides. Aquat. Bot. 90, 172–178.

Genty, B., Briantais, J.-M., Baker, N.R., 1989. The relationship between the quantum yield of photosynthetic electron transport and quenching of chlorophyll fluorescence. Biochim. Biophys. Acta 990, 87–92.

Ghnaya, T., Nouairi, I., Slama, I., Messedi, D., Grignon, C., Abdelly, C., Ghorbel, M.H., 2005. Cadmium effects on growth and mineral nutrition of two halophytes: *Sesuvium portulacastrum* and *Mesembryanthemum crystallinum*. J. Plant Physiol. 162, 1133–1140.

Halliwell, B., Gutteridge, J., 1993. Free Radicals in Biology and Medicine. Clarendon Press, Oxford.

Kalaji, M.H., Loboda, T., 2007. Photosystem II of barley seedlings under cadmium and lead stress. Plant Soil Environ. 53, 511–516.

Krupa, Z., 1988. Cadmium-induced changes in the composition and structure of the light-harvesting chlorophyll a/b protein complex II in radish cotyledons. Physiol. Plant. 73, 518–524.

Krupa, Z., Skórzynska, E., Maksymiec, W., Baszynsky, T., 1987. Effect of cadmium on the photosynthetic apparatus and its photochemical activities in greening radish seedlings. Photosynthetica 21, 156–164.

Krupa, Z., Baszynski, T., 1995. Some aspects of heavy metals toxicity towards photosynthetic apparatus: direct and indirect effects on light and dark reactions. Acta Physiol. Plant. 17.

Küpper, H., Küpper, F., Spiller, M., 1996. Environmental relevance of heavy metal substituted chlorophylls using the example of water plants. J. Exp. Bot. 47, 259–266.

Küpper, H., Seibert, S., Aravind, P., 2007. A fast, sensitive and inexpensive alternative to analytical pigment HPLC: quantification of chlorophylls and carotenoids in crude extracts by fitting with Gauss-Peak-spectra. Anal. Chem. 79, 7611–7627.

Levina, É.N., 1972. General Toxicity of Metals. Meditsina, Leningrad.

Li, W., Khan, M.A., Yamaguchi, S., Kamiya, Y., 2005. Effects of heavy metals on seed germination and early seedling growth of *Arabidopsis thaliana*. Plant Growth Regul. 46, 45–50.

Lindsey, P.A., Lineberger, R.D., 1981. Toxicity, cadmium accumulation and ultrastructural alterations induced by exposure of *Phaseolus* seedlings to cadmium. Hortscience 16, 434.

Liu, S., Yang, C., Xie, W., Xia, W., Fan, P., 2012. The effects of cadium on germination and seedling growth of *Suaeda salsa*. Procedia. Environ. Sci. 16, 293–298.

Marklund, S., Marklund, G., 1974. Involvement of superoxide anion radical in the autoxidation of pyrogallol and a convenient assay for superoxide dismutase. Eur. J. Biochem. 47, 464–469.

Marschner, H., 1995. Mineral Nutrition in Higher Plants, second ed. Academic Press Limited, London.

Marshall, H.J., Geider, R.J., Flynn, K.J., 2000. A mechanistic model of photoinhibition. New Phytol. 145, 347–359.

Martínez-Sánchez, J.J., Conesa, E., Vicente, M.J., Jiménez, A., Franco, J.A., 2006. Germination responses of *Juncus acutus* (Juncaeae) and *Schoenus nigricans* (Cyperaceae) to light and temperature. J. Arid Environ. 66, 187–191.

Mel'nichuck, Y.P., 1990. The Effect of Cadmium Ions on the Cell Division and Plant Growth. Naukova Dumka, Kiev.

Monbet, P., 2004. Seasonal cycle and mass balance of cadmium in an estuary with agricultural catchment: the Morlaix river Estuary (Brittany, France). Estuaries 27, 448–459.

Najeeb, U., Jilani, G., Ali, S., Sarwar, M., Xu, L., Zhou, W., 2011. Insights into cadmium induced physiological and ultra-structural disorders in *Juncus effusus* L. and its remediation through exogenous citric acid. J. Hazard. Mater. 186, 565–574.

Otte, M.L., Bestbroer, S.J., van der Linden, J.M., Rozema, J., Broekman, R.A., 1991. A survey of zinc, copper and cadmium concentrations in salt marshes plants along the Dutch coast. Environ. Pollut. 72, 175–189.

Platt, T., Gallegos, C.L., Harrison, W.G., 1980. Photoinhibition of photosynthesis in natural assemblages of marine phytoplankton. J. Mar. Res. 38, 687–701.

Prodanovic, O., Prodanovic, R., Pristov, J.B., Mitrovic, A., Radotic, K., 2012. Effect of cadmium stress on antioxidative enzymes during the germination of Serbian spruce [*Picea omorika*] (Panč.) *Purkynĕ*]. Afr. J. Biotechnol. 11 (52), 11377–13385.

Przymusiński, R., Rucińska, R., Gwóźdź, E.A., 1995. The stress-stimulated 16 kDa polypeptide from lupin roots has properties of cytosolic Cu: Zn-superoxide dismutase. Environ. Exp. Bot. 35 (4), 485–495.

Rebechini, H.M., Hanzely, L., 1974. Lead-induced ultrastructural changes in chloroplasts of the hydrophyte, *Ceratophyllum demersum*. Z. für Pflanzenphysiol. 73 (5), 377–386.

Reinhold, C., Niczyporuk, S., Beran, K., Jahns, P., 2008. Short-term down-regulation of zeaxanthin epoxidation in *Arabidopsis thaliana* in response to photooxidativestress conditions. Biochim. Biophys. Acta – Bioenerg. 1777, 462–469.

Runcie, J.W., Durako, M.J., 2004. Among-shoot variability and leaf-specific absorbance characteristics affect diel estimates of in situ electron transport of *Posidonia australis*. Aquat. Bot. 80, 209–220.

Sandrini, J.Z., Regoli, F., Fanttori, D., Notti, A., Inácio, A.F., Linde-Arias, A.R., Laurino, J., Bainy, A.C.D., Marins, L., Monserrat, J., 2006. Short-term responses to cadmium exposure in the estuarine polychaete *Laeonereis acuta* (Polychaeta, Nereididae): subcellular distribuition and oxidative stress generation. Environ. Toxicol. Chem. 25, 1337–1344.

Santos, D., Duarte, B., Caçador, I., 2014. Unveiling Zn hyperacumulation in *Juncus acutus*: implications on the electronic energy fluxes and on oxidative stress with emphasis on non-functional Zn-chlorophylls. J. Photochem. Photobiol. B Biol. 140, 228–239.

Stroiński, A., 1999. Some physiological and biochemical aspects of plant resistance to cadmium effect. I. Antioxidative system. Acta Physiol. Plant. 21 (2), 175–188.

Strasser, R.J., Stirbet, A.D., 2001. Estimation of the energetic connectivity of PS II centres in plants using the fluorescence rise O–J–I–P. Fitting of experimental data to three different PS II models. Math. Comput. Simul. 56, 451–461.

Teranishi, Y., Tanaka, A., Osumi, M., Fukui, S., 1974. Catalase activities of hydrocarbon-utilizing *Candida* yeast. Agric. Biol. Chem. 38, 1213–1220.

Thomas, W.H., Hollibaugh, J.T., Seibert, D.L., 1980. Effects of heavy metals on the morphology of some marine phytoplankton. Phycologia 19 (3), 202–209.

Tiryakioglu, M., Eker, S., Ozkutlu, F., Husted, S., Cakmak, I., 2006. Antioxidant defense system and cadmium uptake in barley genotypes differing in cadmium tolerance. J. Trace Elem. Med. Biol. 20, 181–189.

Zhang, X.X., Fan, X.M., Li, C.J., Nan, Z.B., 2010. Effects of cadmium stress on seed germination, seedling growth and antioxidative enzymes in *Achnatherum inebrans* plants infected with a *Neotyphodium* endophyte. Plant Growth Regul. 60, 91–97.

Zhang, X.X., Li, C.J., Nan, Z.B., 2012. Effects of cadmium stress on seed germination and seedling growth of *Elymus dahuricus* infected with the *Neotyphodium endophyte*. Sci. China Life Sci. 55, 793–799.

Zhu, X.G., Govindjee, Baker, N.R., Sturler, E.D., Ort, D.R., Long, S.P., 2005. Chlorophyll a fluorescence induction kinetics in leaves predicted from a model describing each discrete step of excitation energy and electron transfer associated with photosystem II. Planta 223, 114–133.